Clim Dyn (2012) 38:141–160
DOI 10.1007/s00382-010-0969-x

North Atlantic atmospheric circulation and surface wind in the Northeast of the Iberian Peninsula: uncertainty and long term downscaled variability

E. García-Bustamante · J. F. González-Rouco · J. Navarro · E. Xoplaki · P. A. Jiménez · J. P. Montávez

Received: 25 June 2010 / Accepted: 17 December 2010 / Published online: 4 January 2011

Abstract The variability and predictability of the surface wind field at the regional scale is explored over a complex terrain region in the northeastern Iberian Peninsula by means of a downscaling technique based on Canonical Correlation Analysis. More than a decade of observations (1992–2005) allows for calibrating and validating a statistical method that elicits the main associations between the large scale atmospheric circulation over the North Atlantic and Mediterranean areas and the regional wind field. In an initial step the downscaling model is designed by selecting parameter values from practise. To a large extent, the variability of the wind at monthly timescales is found to be governed by the large scale circulation modulated by the particular orographic features of the area. The sensitivity of the downscaling methodology to the selection of the model parameter values is explored, in a second step, by performing a systematic sampling of the parameters space, avoiding a heuristic selection. This provides a metric for the uncertainty associated with the various possible model configurations. The uncertainties associated with the model configuration are considerably dependent on the spatial variability of the wind. While the sampling of the parameters space in the model set up moderately impact estimations during the calibration period, the regional wind variability is very sensitive to the parameters selection at longer timescales. This fact illustrates that downscaling exercises based on a single configuration of parameters should be interpreted with extreme caution. The downscaling model is used to extend the estimations several centuries to the past using long datasets of sea level pressure, thereby illustrating the large temporal variability of the regional wind field from interannual to multicentennial timescales. The analysis does not evidence long term trends throughout the twentieth century, however anomalous episodes of high/low wind speeds are identified.

Keywords Wind · Statistical downscaling · Spatial and temporal variability · Sensitivity · Past reconstruction

E. García-Bustamante (✉) · J. Navarro · P. A. Jiménez
Departamento de Energías Renovables, CIEMAT,
Avenida Complutense s/n, 28040 Madrid, Spain
e-mail: elena.garcia@ciemat.es

E. García-Bustamante · J. F. González-Rouco · P. A. Jiménez
Departamento de Astrofísica y CC. de la Atmósfera,
Universidad Complutense de Madrid, Madrid, Spain

E. Xoplaki
Institute of Geography and Oeschger Centre for Climate Change Research, University of Bern, Bern, Switzerland

J. P. Montávez
Departamento de Física, Universidad de Murcia, Murcia, Spain

1 Introduction

The surface wind field can be loosely considered a local response to the large scale circulation. However, such a response also includes and is sometimes overridden by the effect of orography and a variety of factors such as vegetation, land-sea interactions or other thermally-driven phenomena (Bianco et al. 2006). This combination of large and smaller scale forcings imposes a high spatial as well as temporal variability on the surface wind field (Simpson 1994). The large variability and the vectorial nature of this variable do not only introduce additional complexity to its diagnosis and prediction, but they also provide the topic with a valuable scientific interest. The analysis and prediction of the wind field variability at different timescales comprise practical applications that range from the short

term wind forecasting to the assessment of climatological wind variability changes: storms forecasting (Powell et al. 1991), air pollution (Jakobs et al. 1995) and surface roughness studies (Grimenes and Thue-Hansen 2004), structures design related to extreme wind events (Zhang et al. 2006) or wave field evaluation (Caires and Sterl 2004). Beside those relevant to society applications, in the context of renewable energies, special attention is being paid to the wind power prediction at short timescales (Kariniotakis et al. 2004) as well as the medium/long term wind predictability evaluation applied to the resource assessment (Pryor et al. 2006, 2009).

The improved understanding of the regional/local wind variability and its relation to the large scale atmospheric circulation, greatly benefits applications targeting at wind related variables prediction. Assessments of climate variability at the regional scale are mainly based on the application of *downscaling* approaches that employ large scale atmospheric circulation information to obtain estimations of variables at the regional/local scale by identifying the main statistical associations between the spatial scales (statistical downscaling) or using limited area models (dynamical downscaling). The large scale atmospheric state is provided by gridded observations (Zorita et al. 1992; Zorita and von Storch 1999), reanalysis data (Xoplaki et al. 2003a, 2004) or general circulation model (GCM) outputs (Lenderink et al. 2007).

The statistical downscaling consists in training a statistical model making use of the empirical relationships observed between the local variables, *predictands* and the large scale atmospheric variables, *predictors* (González-Rouco et al. 2000; Xoplaki et al. 2004; Busuioc et al. 2008). In the context of wind field related studies, Kaas et al. (1996) identified the connection between SLP/SST patterns and the local wind field in winter over Scandinavia and Pryor and Schoof (2005) and Pryor et al. (2005b) proposed an empirical downscaling using the outputs of a set of GCMs and estimated variations of the parameters of a typical wind probability distribution at the regional scale in northern Europe. In turn, the dynamical downscaling is based on the use of regional circulation models (RCMs) that solve the fundamental equations of the atmosphere yielding finer time-space simulations (Hong and Kalnay 2000; Conil and Hall 2006). Some examples in the context of wind field analysis are those of Pryor et al. (2005a) that studied the implications of the long term wind variability for the wind energy resources over northern Europe using RCMs and Jiménez et al. (2010b) who evaluated the ability of a RCM to identify subregions with similar wind behaviour, previously found with observations from the same area in the northeast of the Iberian Peninsula (IP). Some studies focused on the regional scale also employ a combination of both strategies (de Rooy and Kok 2004). Besides, an extended application of the downscaling techniques consists in forcing the dynamical or statistical model with large scale fields obtained from future climate change GCM projections (Denman et al. 2007).

However, the transfer of information between spatial scales involves many sources of uncertainty that propagate from the global to the regional scale in the downscaling exercises (Mitchell and Hulme, 1999; Schwierz et al. 2006). In the context of future climate projections, the uncertainties associated with the radiative forcing are accounted for by considering a variety of climate change scenarios (Nakicenovic et al. 2000; Denman et al. 2007) and by the use of a suite of GCMs to represent the intermodel variability. Pryor et al. (2006) studied the possible changes of surface winds in northern Europe through the downscaling of several GCM simulations under different scenarios. Najac et al. (2009) applied a statistical downscaling to a multi GCMs ensemble and estimated future changes of the wind field over France in a particular future climate scenario. The uncertainty associated with the use of a specific model for the downscaling step can also be addressed. In the case of RCMs, the effect of changes in the discretization of the equations of motion or the different parametrizations can imply changes that contribute to the uncertainty in the simulated regional field. Experiments that explore the sensitivity of the model to variations in the physics (Zhang and Zheng 2004) or to changes in the initial conditions (Weisse and Feser 2003) are designed to provide a measure of this type of uncertainty. In the case of statistical methods, the effect of applying different methodologies can also be examined (Zorita and von Storch 1999; Matulla et al. 2003; Maurer and Hidalgo 2007). Even in the case of using one specific downscaling method, uncertainties arise from a number of somewhat subjective decisions taken in the design of the statistical model. Usually such decisions are founded on good practise and lead to skillful estimations of the target regional variables (Hanssen-Bauer et al. 2005). However, introducing changes in the model configuration by changing parameter values, spatial domains, etc., would produce somewhat modified, though still skillful, estimations. Even in the case of methods that provide probabilistic estimations of the regional targets (Fernández et al. 2007; Furrer et al. 2007; Dibike et al. 2008) there are additionally unquantified uncertainties stemming from specific decisions in the model set up. These additional uncertainties are difficult to estimate, but they can at least be explored considering a variety of configuration designs in the downscaling approach. This path illustrates the sensitivity to changes in the model configuration, what can be regarded as a methodological variability or methodological uncertainty. Interesting works in this context are carried out by Huth (2000, 2004) who investigated

the sensitivity of local downscaled temperatures in Central Europe to changes in the predictor variables. Nevertheless, this type of studies are rather uncommon in the case of wind related variables, thus an exploration of the methodological sensitivity of statistically downscaled wind field seems pertinent. Furthermore, the uncertainty may also arrive from potential inaccuracies of the GCMs or reanalysis as they provide the large scale information that feeds the downscaling models. For this reason, it is also interesting to explore the uncertainty that is associated with the use of different datasets as boundary and initial conditions in the case of the dynamical downscaling (Koukidis and Berg 2009) or as predictors if dealing with statistical models. Notwithstanding the evaluation of the different sources of uncertainty affecting the regional scale is an issue under development (Denman et al. 2007).

This work aims at analysing the statistical downscaling relationships between the large scale atmospheric circulation and the local wind field in a region located in the northeastern IP. Almost fourteen years of monthly observations are used to calibrate a statistical model that isolates the most important circulation patterns for the wind field at regional scales. The model applied is based on the Canonical Correlation Analysis (CCA). A specific selection of parameters in the design of the model is used to explore the variability of the regional wind field. In order to further assess the uncertainties associated with the regional estimates, the effect of variations of the model parameters is explored providing insight into the methodological sensitivity. The parameters involved in the model configuration that are investigated in this step are, for instance, the size of the geographical domain of the large scale predictors or the number of canonical modes retained for the analysis. The uncertainty that arises from the use of different datasets as large scale predictors (reanalysis data, observations or climate field reconstructions) is also evaluated. The combination of both sources of uncertainty will provide a more reliable estimation of the wind field variability. An additional benefit of obtaining a measure of the uncertainties that arise in the downscaling step implies that in subsequent stages of the work they could be compared to those derived from the use of different GCMs in future climate change projections or those coming from the use of different scenarios. In such conditions a representation of the full cascade of uncertainties involved in future regional climate projections would be feasible.

The understanding of the mechanisms responsible for the temporal variations of the regional wind at interdecadal and centennial timescales is hampered by the limited temporal length of the observational series since usually short periods are used for calibrating and validating models. For this reason wind estimations and their associated uncertainty are downscaled several centuries backward using available datasets of large scale predictor variables. The long term variability of the regional wind is interpreted in terms of the variations in sign and intensity of the main modes of the atmospheric circulation affecting the regional wind that were found during the calibration period. This exercise provides a broader perspective of the regional wind variability in observations that may be of use in the context of comparison with climate change downscaling exercises.

The downscaling methodology applied herein (Sect. 3) is focused on a region in the northeast of the IP (Sect. 2), thereby providing the possibility of assessing not only the role of large scale circulation forcings but also the non negligible influence of regional/local factors. A reference configuration of the downscaling model is fixed to analyse its skill and the modes of coupled large to regional scale variability (Sect. 4) The sensitivity of changes in the reference configuration is explored in Sect. 5 and used to extent our knowledge of the wind variability in the region several centuries back using a set of available large scale predictors (Sect. 6) The results described in the following sections have therefore implications for the understanding of regional wind variability, the design of the downscaling strategies and the understanding of the associated uncertainties. This last feature can be of particular value applications within the context of downscaling of climate change scenarios projections. This work offers the reader new perspectives, that to the knowledge of the authors, are not documented in the literature.

2 Data

2.1 Large scale predictors

Six gridded (2.5° latitude × 2.5° longitude) variables over the North Atlantic region and Europe are used as predictor fields for the CCA exercise: sea level pressure (SLP), 850 and 500 hPa geopotential heights (ϕ_{850} and ϕ_{500}), 10-m height zonal (U10) and meridional (V10) wind components and 500–850 hPa thickness data ($Z_{500-850}$). Monthly mean values are calculated from the original 6-h resolution time series. Data are taken from the ERA-40 reanalysis of the European Center for Medium-Range Weather Forecast (ECMWF; Uppala et al. 2005) from 1992 to 2002. Analyses from the ECMWF global model outputs are also used to complete the whole period of observations (2002–2005); for the sake of simplicity this database will be referred to as the ERA-40 fields from now on. The strategy of combining both ERA-40 and the ECMWF datasets has been used previously in other studies as in Fisher et al. (2007) or in

Jiménez et al. (2010b). Jiménez et al. (2010b) performed a numerical simulation of the wind field using both datasets as initial and boundary conditions over the same target region and period. No evidences of inhomogeneities due to the use of the two forcing datasets were found, thus, it appears reasonable to use the same set up to overcome the lack of reanalysis data after 2002.

For two additional exercises that (1) explore the uncertainty related to the use of different datasets as large scale predictors (Sect. 5.2) and (2) provide a wind field past reconstruction (Sect. 6), only one variable, the SLP from different sources with longer temporal coverage, is used. The datasets employed in these two parts of the work are: (a) monthly SLP observations from 1899 to 2005 from the National Center for Atmospheric Research (NCAR; Trenberth and Paolino 1980); (b) an observational dataset provided by the Hadley Centre consisting of historical gridded monthly mean SLPs (HadSLP2) for the period 1850-2004 (Allan and Ansell 2006); and (c) a SLP proxy-based reconstruction from 1659 by Luterbacher et al (2002). This reconstruction is limited to a spatial domain ranging from 30°W to 40°E in longitude and from 30°N to 70°N in latitude. The information regarding the large scale predictors used in this work is summarized in Table 1.

2.2 Observed wind field: predictand

The area under study is the *Comunidad Foral de Navarra* (CFN) in the NE of the IP, a small region of intricate orography surrounded by two large mountain ranges, the Pyrenees and the Cantabrian systems. Many other smaller geographical features give rise to a complex landscape of the region (Fig. 1). It is worth noting the presence of the Ebro Valley, which is bounded by the Pyrenees and the Iberian mountain ranges and spreads out to the south following a NW-SE axis. These orographic elements will evidence a strong impact on the behaviour and predictability of the wind field.

The wind observations over the CFN were measured at 29 meteorological stations from January 1992 to September 2005. Their geographical distribution is represented in Fig. 1. The original measurements were subject to quality control analyses (Jiménez et al. 2008b, 2010a). In addition, observational data from 3 wind farms in the CFN (squares in Fig. 1) are also used for this study. These wind series span throughout the period between June 1999 and May 2003, for the longest series. Their inclusion in the analysis is interesting to illustrate the influence of the orography by comparing these wind farm records obtained at the hub height (between 30 and 40 m) and usually at the top of a hill with the wind measured at the rest of stations, located closer to the surface (at 10 m and a few of them at 2 m, see caption in Fig. 1). These datasets have been already used in other studies that explored the variability of the wind field in the region (Jiménez et al. 2008a, 2008b) and the relation to wind power production at the wind farm locations (García-Bustamante et al. 2008, 2009).

The present study is focused on the most windy months, when the links between the atmospheric circulation and the regional wind field are stronger. In autumn and winter the surface pressure gradient over the Ebro Valley is intensified and stronger winds are associated with an intense cold air advection from the Atlantic area (de Pedraza 1985; Jiménez et al. 2008a). For this reason an extended *winter* season covering September to March is used in this analysis.

The climatology of the wind field in the region is described in the following paragraphs. Observed mean wind module (solid curves) and wind components (vectors) are represented in Fig. 2. The mean flow in the CFN is from NW to SE and it is channeled from the northern valleys along the Ebro Valley (Jiménez et al. 2008a). This is a characteristic cold and dry wind pattern in the CFN region known as *Cierzo*. The flow in the opposite direction (SE to NW) is known as *Bochorno*, resulting from the advection of moist and warmer air from the Mediterranean. The dashed lines in Fig. 2 show the standard deviation of the wind module. As it is shown, the spatial variations of wind and its deviation are coincident to a good degree, which is a typical feature of positively defined variables like precipitation (Xoplaki et al. 2004). It is worth noting that some locations at the north and centre of the region reveal a higher mean wind than the rest of the sites. Some of these sites correspond to the wind farms, located at higher elevations with anemometers at around 40 m a.g.l.,

Table 1 Characteristics of the datasets employed as large scale predictors: source and data type, variables considered within the dataset, period used for the analyses and spatial resolution (° lat. x ° lon.)

Source	Type	Variables	Period (years)	Spat. res.
ERA-40	Reanalysis/analysis	SLP,$\phi_{850,500}$,UV10,$Z_{500-850}$	1957–2005	2.5° × 2.5°
NCAR	Observations	SLP	1899–2005	5° × 5°
HadSLP2	Observations	SLP	1850–2004	5° × 5°
Luterbacher et al. (2002)	Reconstruction	SLP	1650–1999	5° × 5°

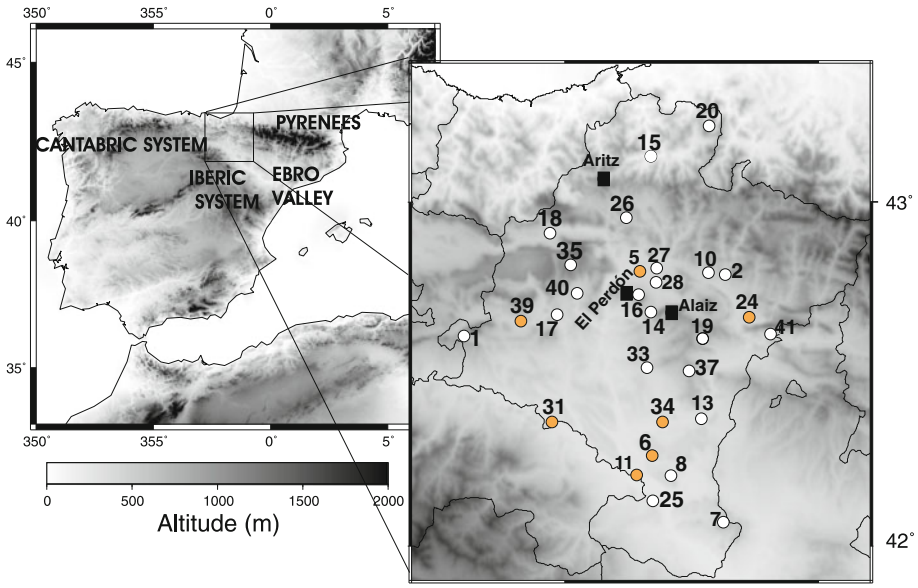

Fig. 1 Location of the wind stations (*white circles*) in the CFN. Each site is labeled with the same number as in Jiménez et al (2008b). The reader is addressed to Table 1 therein for further details about site descriptions. *Coloured circles* stand for those stations with anemometers at 2 m while the rest are located at 10 m height. Squares correspond to the wind farms locations: Aritz, El Perdón and Alaiz (García-Bustamante et al. 2008). Shading illustrates the orography of the region

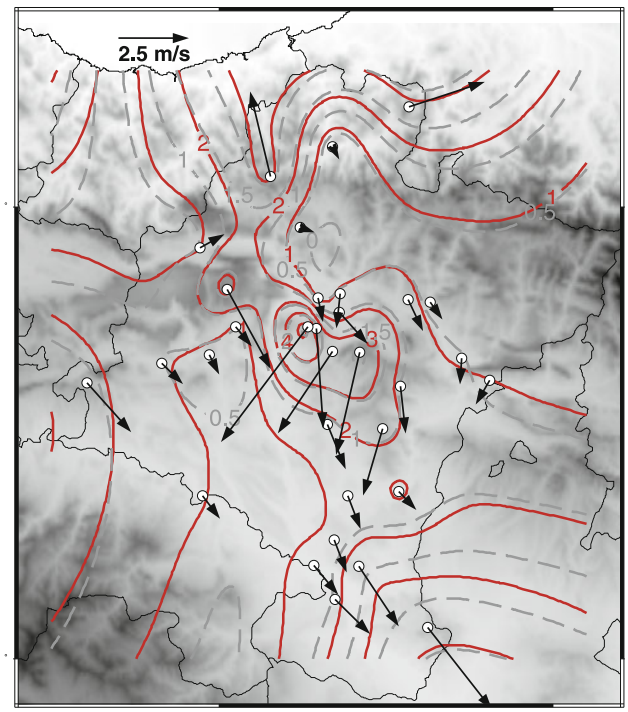

Fig. 2 Observed mean zonal and meridional wind components (vectors) and wind module (*red solid contours*). Dashed contours show the spatial variations of the wind module standard deviation

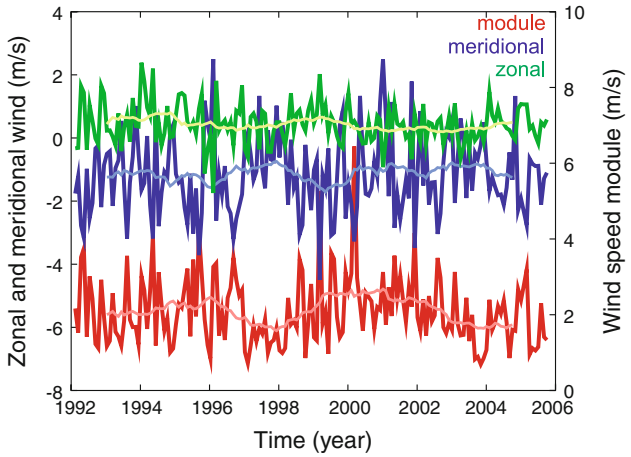

Fig. 3 Regional zonal (*green*) and meridional (*blue*) wind components and wind module (*red*) throughout the whole observational period. The corresponding 3 years moving average is also represented

less influenced by smaller scale orographic features. Two of the wind farms show a more NE-SW flow in agreement with the mean direction at the surrounding stations while the other, more northerly located, presents a more SE-NW direction. In fact, the northern area in the CFN is exposed to a different large scale circulation regime than the central and southern sections of the region under study (Jiménez et al. 2008b).

The spatially averaged, hereafter the *regional*, time series of the zonal and meridional observed wind components and wind module are represented in Fig. 3. It can be appreciated that, for the wind components, series present opposite sign throughout the whole period. Their correlation value is −0.77. This suggests a conservation of the surface momentum between both wind components at these timescales (Jiménez et al. 2008b). Changes in the wind module (Fig. 3) present substantial intra and inter-annual variability which could be of great interest, e.g, in the context of wind energy assessment.

3 Downscaling methodology

The statistical method applied in this study is based on CCA. This is a multivariate statistical technique that

isolates linear associations between sets of predictor and predictand variables that are optimally correlated (Hotelling 1935, 1936; Glahn 1968; Levine 1977). The original data are projected onto their principal components (PCs) to remove noise and reduce the number of degrees of freedom. The methodology is further described in von Storch and Zwiers (1999).

Before calibrating the model, the annual cycle is removed by subtracting the monthly climatological mean to obtain anomaly fields. Time series were also detrended applying a linear least square fit in order to ensure the long-term stationarity (Xoplaki et al. 2003b). In order to account for the latitudinal distortions, anomalies from the large scale fields were weighted at each grid point by multiplying by the square root of the latitude to consider the decreasing size of grid boxes with the variations in grid box size with latitude (North et al. 1982b). Additionally the time series were standardized (dividing by their standard deviation). Both predictor fields were combined to perform a joint EOF analysis. The size of the matrices allowed for managing the problem in a single step. Eventually, the same number of modes from both predictor EOFs were retained, as they accounted for a similar amount of explained variance, for the posterior combined CCA (Preisendorfer 1988; von Storch and Zwiers 1999).

A certain combination of the model parameters was selected in a first step of the analysis. This selection does not correspond to the optimal case, although it generates reasonable estimates of the wind field. This selection, prior to the sensitivity analysis, represents a standard situation (thereafter called *reference case*) to illustrate the potential of the methodology and allows for understanding the emergent associations between predictors and predictands. The choice of parameters for this reference case is exposed in Sect. 4.1. However, variations in this selection and their influence on the results will be explored in the sensitivity analysis in Sect. 5.

After the design of the downscaling model, its skill is verified using a crossvalidation approach. This allows to reduce a possible overfitting of data by the model (Barnett and Preisendorfer 1987). The crossvalidation is a resamplig technique in which a small number of data is dismissed and the model is trained with the retained data subset. The removed values are then estimated with the calibrated model. This procedure is repeated recursively by sampling subsets of the same length along the entire observational record in order to obtain a full set of independent estimates that are compared afterwards to the original observations (Michaelsen 1987). Further details on the size of the sampling subsets are given in the following sections.

The actual extended winter season dataset analysed herein is composed of 91 monthly wind observations at each site (14 years $\times$ 7 months/year) and thus hardly spans more than a decade. It can be argued this is a limitation for the analysis and should not be forgotten in the interpretation of results since the model is calibrated making use of intraseasonal to decadal cross-covariances and it is assumed to reproduce wind variability at multidecadal and even centennial timescales. This assumption is however not alien to downscaling approaches where the best use of available data has led in some analysis to calibrate models based on comparatively short decadal records (Huth 2002, 2004; Gerstengarbe and Werner 2008) or, in a more typical approach, to use multidecadal long records to estimate variability on centennial and longer timescales (e.g., González-Rouco et al. 2000; Xoplaki et al. 2003a). On the other hand, the afore mentioned crossvalidation approach contributes to ensure the robustness of the statistical relationships and reduces possible overfitting of data (Barnett and Preisendorfer 1987).

To evaluate the predicting skill of the method, the correlation coefficient (ρ) and the Brier Skill Score (β) have been used in this work. ρ yields a measure of the temporal concordance between the observations and estimations. β provides a measure of the variance of observations that is accounted for by the model. This coefficient is defined as $\beta = 1 - [S^2_{ES}/S^2_{OB}]$, were S^2_{ES} represents the variance of the estimations error and S^2_{OB} is the observations variance, provided that the climatology is selected as reference value to evaluate the error. In such conditions $\beta = 0$ represents a prediction not better than climatology. If the estimations error variance is similar to that of the observations a positive β is obtained (the better the prediction, the closer to 1).

4 Wind estimations in the CFN: the reference case

In this section results from the calibration of the statistical downscaling model are presented (Sect. 4.1) and evaluated (Sect. 4.2). This will serve as a reference configuration hereafter. Monthly zonal (west–east) and meridional (north–south) components of the wind are employed as predictand fields.

In the reference case two ERA-40 fields (see Sect. 2.2), ϕ_{850} and $Z_{500-850}$, are used as predictors as they provide a dynamical and thermal description of the atmospheric circulation. The analysis is limited to a geographical area spanning from 35°*N* to 65°*N* and 40°*W* to 10°*E*. 4 predictor *EOFs* are retained for the analysis, accounting for a 81.5% of the total variance. The same number of *EOFs* is considered for the predictand that account for a 90.2% of the variance. 2 pairs of canonical modes are retained in the design of the downscaling model. In the reference configuration the size of the crossvalidation sampling subset is one month. This selection does not necessarily correspond

to the optimal case. The choice of model parameters is based on a prior heuristic exploration of several model configurations, as a previous step to the sensitivity analysis, to gain some insight about the variance within estimates due to changes in the model parameters. Thus, this configuration was selected for illustration purposes and provides estimations in good agreement with observations. In Sect. 5 variations of this reference configuration will be explored.

4.1 Canonical patterns and series

The first pair of canonical patterns (CCA1) is represented in Fig. 4a, b for the predictor and predictand variables, respectively, together with their amplitude time series or *canonical coordinates* (Fig. 4c). The large scale pattern (Fig. 4a, shaded for ϕ_{850} and contours for $Z_{500–850}$) depicts a dipole structure with positive anomalies over the North Atlantic area, that reaches the west side of the IP. Negative anomalies are located northeast of the British Isles, centred over the Scandinavian Peninsula. The simultaneous CCA1 pattern for the predictand (regional wind) presents in its positive phase a NW-SE wind anomaly pattern which can be related to the well known regional '*Cierzo*'. It should be noticed that the reverse sign of the patterns is also possible since it is determined by the sign of eigenvalues of the cross-covariance matrix (von Storch and Zwiers, 1999). Therefore, the negative phase of this mode presents contributions to the flow from the SE with relatively warm and moist air advection from the Mediterranean that can be regarded as the typical '*Bochorno*'. The two patterns are physically meaningful provided that the large scale mode induces a pressure gradient that favours a NW-SE (SE-NW) direction for the geostrophic wind. In addition, the axis of the Ebro Valley, aligned with this NW-SE direction, contributes with a strong channeling effect at the surface. Thus, the local wind pattern arises as a result of the large scale atmospheric structure modulated by the orographic configuration of the CFN. This first mode accounts for 18% (22%) of the total variance of the ϕ_{850} ($Z_{500–850}$) predictor field and around 36% of the total predictand variance (see Table 2 for summarized information on correlations and explained variances). The same large scale regime as found here, that causes a partial blocking of the westerlies, has been associated with the Mistral conditions (Buzzi et al. 2003; Burlando, 2009). Thus, this large scale pattern is

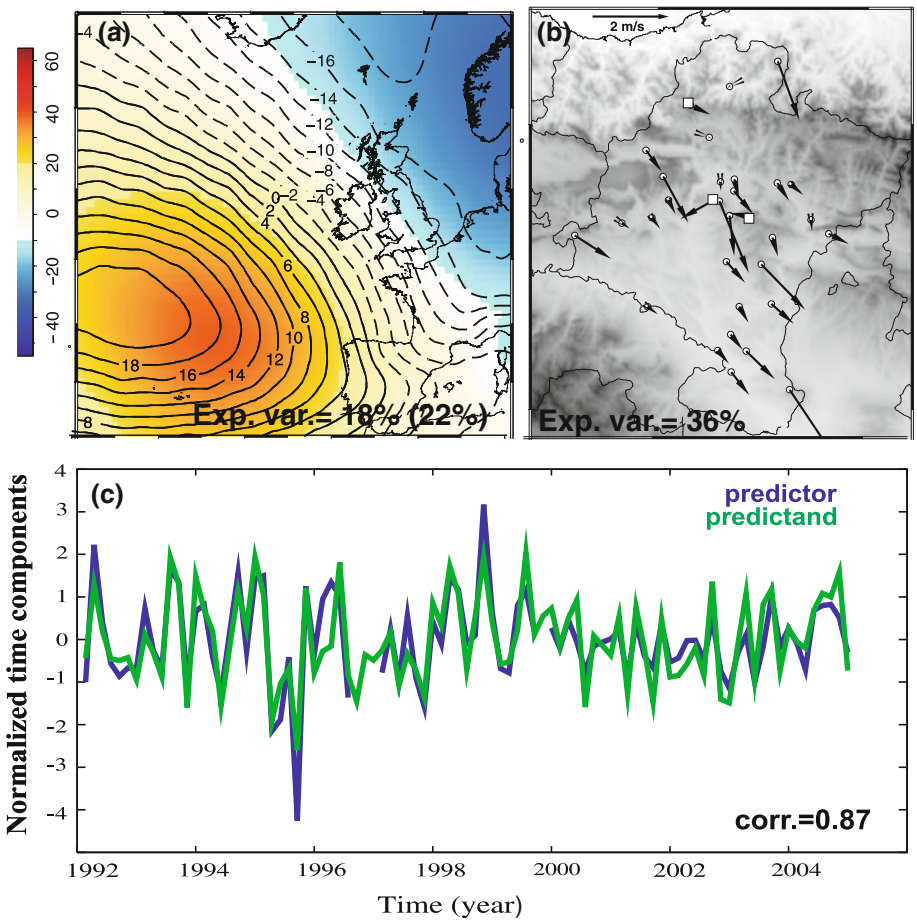

Fig. 4 Canonical patterns and series of the first CCA mode (CCA1). **a** Predictor patterns, ϕ_{850} hPa (*shaded*) and $Z_{500–850}$ hPa (contours); the explained variance of the ϕ_{850} ($Z_{500–850}$) field is also indicated; **b** predictand (local wind in the CFN) pattern together with the variance accounted for by this mode; wind farms are represented with white squares. **c** Canonical series for predictor (*blue*) and predictand (*green*)

Table 2 Canonical correlations and explained variances by the CCA modes

	Corr.	$\phi_{850}/Z_{500-850}$ expl. var. (%)	Predictand expl. var. (%)
CCA1	0.87	18/22	36
CCA2	0.86	30/13	36

broadly responsible for predominant meridional circulations not only in the region under study, but also in wider areas over the European continent.

The corresponding amplitude series for predictor and predictand (Fig. 4c) present a canonical correlation of 0.87 and exhibit considerable intra and interannual variability with extreme values at the end of 1995 and 1999. The variability is higher till 2000 and slightly lower in the following period. As this change in the regional wind variance during the last period is also noticeable in the predictor series, it can be attributed to changes in the large scale circulation variability. The canonical series of the local wind components presents a correlation of 0.92 and −0.83 with the regional time series of the observed zonal and meridional wind components (Fig. 3), respectively. Thus, this first canonical mode describes the most important changes in regional monthly wind variability for the period studied.

The second pair of coupled patterns (CCA2) shares 30% (13%) of variance of the ϕ_{850} ($Z_{500-850}$) field and 36% with the regional wind or predictand. The canonical predictor mode consists of a monopole pattern of negative anomalies centred westward of the British Isles. This pattern in its positive phase indicates a zonally eastward oriented geostrophic flow. The CCA2 wind pattern (Fig. 5b) shows a configuration with a more zonal direction at most of the windiest sites over the northern and centre part of the region, that coincide with the wind farm locations. These sites are more exposed to quasi-geostrophic circulations and less affected by local scale phenomena. For the rest of stations, the surface wind field displays a SE-NW direction which is coherent with a deflection of the geostrophic wind that tends to balance the horizontal pressure gradient and helps to introduce southern surface flows in the valley mouth. Hence, this mode in its positive (negative) phase evidences contributions to the *Bochorno* (*Cierzo*). This coupled mode shows a decisive impact of the orography, contributing for instance to circulations that are prone to be channeled along the Ebro valley due to the strong orographic constraint. It additionally evidences an important influence of the large scale circulation since some stations in central and northern CFN or the wind farm locations, which are not subject to the channeling effect at the valley, show a more zonal response to that mode. The correlation between the CCA2 time components is 0.86 (see Table 2). They show large intensity contributions in 1993 and during the period between 2000 and 2002 and also reveal a considerable intra and interannual variability.

It is well worth to discuss the relation of the canonical large scale modes with the main teleconnection patterns in the Atlantic area. The Iberian Peninsula and especially the CFN, is geographically located at the boundaries of the storm track in the North Atlantic region and potential fluctuations of the different modes over the climate of the region can be expected (Seierstad et al. 2007). In Table 3, the correlations between the first two canonical series of the predictor fields and the indexes of the teleconnection patterns are given (Barnston and Livezey, 1987).[1] Most of the correlation values are significant at a 0.05 level (in bold). However, the highest correlation with the CCA1 large scale pattern is found with the East Atlantic/Western Russia mode (EA/WR; Burlando 2009). In the case of the CCA2, the strongest relation is found for the East Atlantic pattern (EA). The low correlation identified between the canonical series and the NAO index points to the influence of the orography on the wind fields that is responsible of more meridional flows as suggested also in Fernández and Saenz (2003), that find comparable canonical modes in their analysis of winter precipitation on the northern coast of the Iberian Peninsula. Similar cases are also the Tramontana and Mistral winds (Burlando 2009), that are not favoured by NAO-like circulations but by large scale modes connected with meridional flows, channeled and accelerated along the natural mountainous pathways.

4.2 Validation of wind estimates

The estimated regional anomalies for the zonal and meridional wind components and wind module are compared to their observational counterparts in Fig. 6. The correlations between the regional estimations and observations are 0.79 and 0.80 for the zonal and meridional component, respectively and 0.70 for the wind module (all correlations are significant at a 0.05 level). The lower correlation of the wind module can be understood on the basis of the non-linear transformations applied to obtain it from the wind components together with the potential accumulation of the errors from each component. The higher variability of the meridional component becomes evident again. It can be observed that the estimations show also reduced variance with regard to the observations. This loss of variance is inherent to the linear methodologies (von Storch and Zwiers 1999).

The skill of the method at each station is evaluated through the values of ρ and β represented in Fig. 7a–c. This inspection allows for a validation of the procedure at

[1] http://www.cpc.ncep.noaa.gov/data/teledoc/telecontents.shtml.

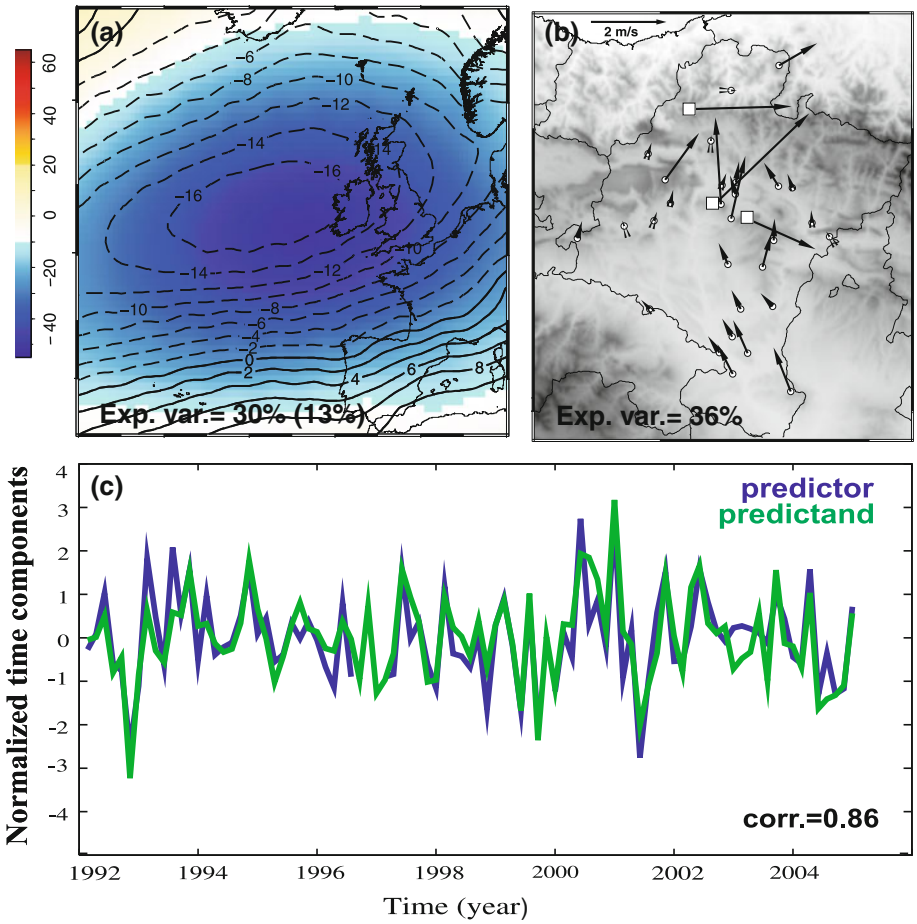

Fig. 5 As in Fig. 4 but for the second CCA mode (CCA2)

Table 3 Correlation values between the two first canonical series and the main teleconnection patterns over the Atlantic area: North Atlantic Oscillation (NAO), East Atlantic Pattern (EA), East Atlantic/Western Russian pattern (EA/WR) and the Scandinavian pattern (SCAN)

	NAO	EA	EA/WR	SCAN
CCA1	0.16	**0.28**	**−0.47**	**−0.32**
CCA2	**−0.24**	**0.46**	**0.20**	**0.27**

Bold values are significant at 0.05 level

the local scale providing an overview of the predictability depending on the specific location. The size of circles is proportional to the correlation (ρ) value and the color is related to the Brier skill score (β). At most of the locations the correlation values range from 0.85 to 0.50 for both wind components. Also the Brier skill score shows a reasonably good performance of the model in terms of the variance error (values span the interval 0.72–0.30). A few locations at the northern areas and some stations at the mainland valleys show a decay of the skill in both their ρ and β values. These stations are located in less windy sites (Fig. 2) or in areas with more complex orography that contributes to a decrease of the predictability. Overall, the pattern is very similar for both components but higher scores can be observed along the NW-SE axis of the Ebro Valley for the meridional one. The main differences between them are found in the northern and the mountain stations, where the zonal component predictability is slightly deteriorated. The wind module as in the case of the regionally averaged series shows also slightly worse performance compared to the two wind components.

The Taylor diagram (Taylor 2001) in Fig. 7d illustrates the behavior of the regional estimations compared to the performance of the wind estimates at each location. This is a polar diagram where the angle is indicative of the correlation value and the radial coordinate accounts for the standard deviation between estimations and observations at each location. Green (blue) points correspond to the zonal (meridional) component of the wind for each site whereas the red dots correspond to the wind module. It is worth noting that the regional average time series (squares) tend to outperform the cloud of points. The regional estimates filter out many local effects that in some cases cannot be well captured by the downscaling model and reinforce the signal to noise ratio. This is especially the case of the meridional component of the wind that is characterized by

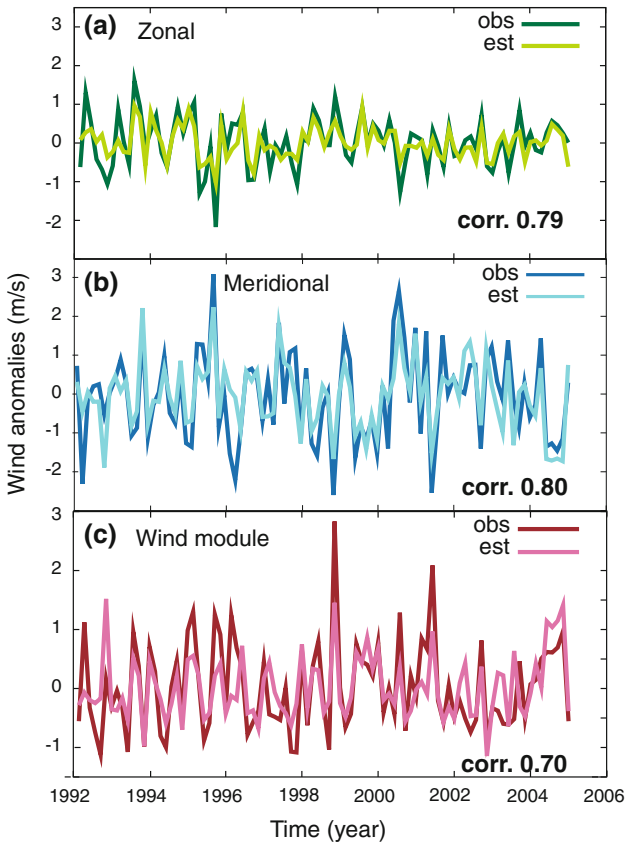

Fig. 6 Regional observed and estimated monthly zonal (**a**) and meridional (**b**) wind components as well as wind module (**c**) anomaly time series

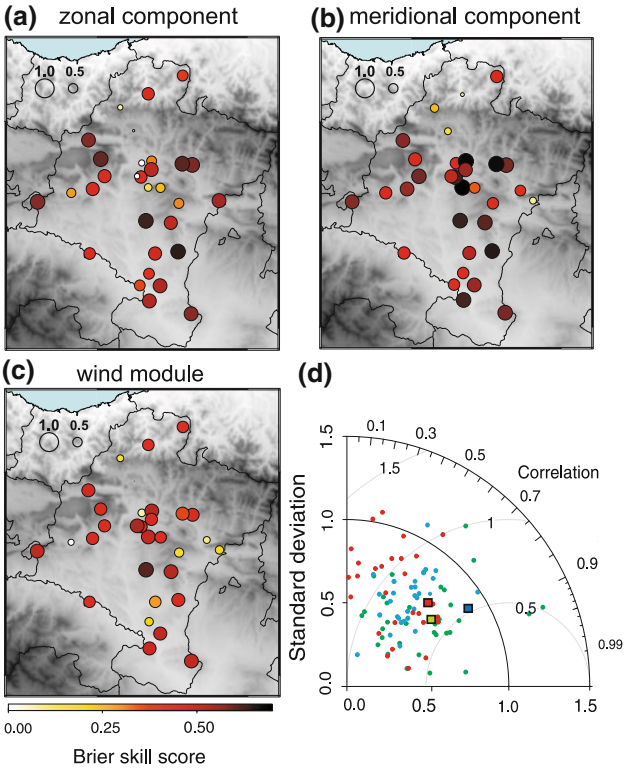

Fig. 7 Correlation and Brier skill scores calculated between the wind observations and estimations for **a** zonal, **b** meridional wind component and **c** wind module. **d** Taylor diagram for each wind component (*green* is zonal and blue meridional) and for the wind module (*red*) for each time series (points). The corresponding regional (spatial average of all time series) scores are represented with *squares*

showing common variability in the whole region of study (Jiménez et al. 2008b).

On the basis of the results above, hereafter, the discussion of the method performance will be restricted to the wind components.

5 Uncertainty analysis

In this section an evaluation of the uncertainties associated with the statistical downscaling model is presented. The methodological sensitivity is assessed in order to evaluate to what extent a certain choice of parameters in the set up of the experiment produces an impact in the estimations, thus exploring the robustness of the downscaling strategy. The approach consists in allowing a certain degree of variability in each parameter that is important for the model configuration. The sampling of the parameters space is accomplished in two subsequent steps. First, variations in each parameter with respect to the reference model are allowed keeping the others fixed. This variation of parameters generates a family of estimates that will allow for an assessment of the spatial variability of the method sensitivity to changes in one specific parameter. Second, all parameter values are systematically varied in a large amount of model configurations that allow for any parameter combination (see Table 4). By doing so the temporal evolution of the method sensitivity will be studied.

Table 4 Parameters of the model configuration and number of options considered for each one

Parameter	*n*° options
Predictor domain	9
Predictor field	25
n° EOFs/CCAs	31
Crossval. subset	9
Total *n*° experim. 1 param. varying	74
Total *n*° experim. all params. varying	62.775

The two last rows correspond to the total number of experiments (note that the penultimate row is the result of the sum of the number of options when a single parameter is allowed to vary and the last row corresponds to the case where changes in all parameters are combined)

The uncertainty derived from the large scale adds on top of the cascade when evaluating the regional estimations of climate variability. In this context, it is also interesting to evaluate the impacts of using large scale predictors from different datasets. The differences between datasets are connected to their nature, for instance whether they are observations, global model outputs or reconstruction data or to the methodologies applied to obtain these datasets for instance, the quality control procedures, their validation, interpolation schemes, etc. This type of uncertainty is explored in Sect. 5.2.

5.1 Methodological uncertainty

The parameters of the model configuration that are systematically sampled are: (a) the size of the large scale domain, tested by using different windows that cover from smaller areas over the target region to larger windows over the northern Atlantic and Mediterranean areas; (b) the predictor field, considered by examining several dynamical and thermal variables and/or combinations of them; (c) the number of EOFs and CCAs retained for the analysis and (d) the size of the crossvalidation subsets, exploring cases where this changes from 1 month to 4 years (28 months). The crossvalidation option is not a decisive parameter of the downscaling method since it does not affect the associations between the large scale circulation and the regional wind. However changes of the crossvalidation subset length should not affect an assessment of the quality of estimates. Thus, it is interesting to test the robustness of the validation process to variations in the crossvalidation option. The number of options for all parameters is summarized in Table 4.

Nine large scale windows (Fig. 8; plotted for illustration over the ERA-40 SLP mean field) are analysed with the aim of understanding and illustrating the effect of the spatial domain on the estimations. The window corresponding to the reference case is number 4 in this figure. Regarding the predictor field(s) the variables considered are: SLP, ϕ_{850}, ϕ_{500}, the $Z_{500-850}$ and the UV10 fields (de Pedraza 1985) together with all possible combinations of two or three of these fields. The number of retained EOFs for the analysis varies between 2 and 6. The maximum (6) was determined by including all the statistically significant correlations between the predictor and predictand principal components (PCs). This can be seen in detail in Fig. 9a where the coloured matrix shows the correlation values between the first six predictor and predictand PCs (significant correlations at 0.05 level are marked with a circle). For the minimum number of EOFs a criterion based on the variance that the leading EOFs account for is considered. This minimum is determined by the presence of a breakpoint in the curves of Fig. 9b (explained variance *vs*. number of EOFs/CCAs) which is an indicator of the modes that should be included in all the experiments since they contain the most significant amount of explained variance. In the case of the predictor, the minimum number of EOFs is 2. This implies a 57% of explained variance. For the predictand the breakpoint occurs also at the second EOF (almost a 80% of explained variance). The selection of the number of EOFs can be also done with more sophisticated methods although there is no optimal criterion for it (Kaiser 1960; North et al. 1982a; Preisendorfer 1988). In the case of the number of CCAs, the maximum is imposed by the maximum number of EOFs retained, since the number of CCA modes must be equal or smaller than the smaller (predictor or predictand) number of EOFs (Barnett and Preisendorfer 1987). Although the maximum was 6 only the first four canonical patterns presented significant correlations. The minimum is set to 2 with

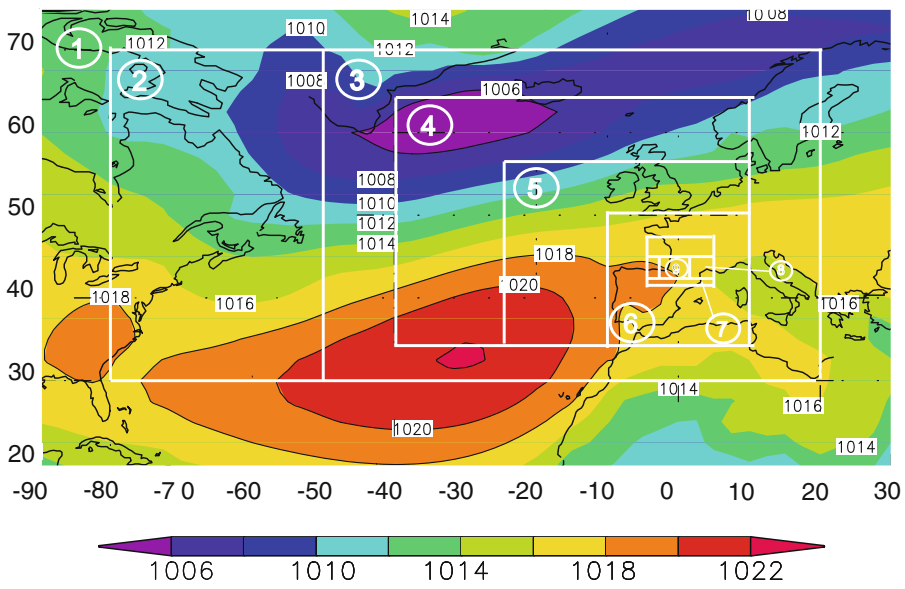

Fig. 8 Different large scale domains together with the mean field of one of the predictor variables (ERA-40 SLP) considered for the sensitivity analysis

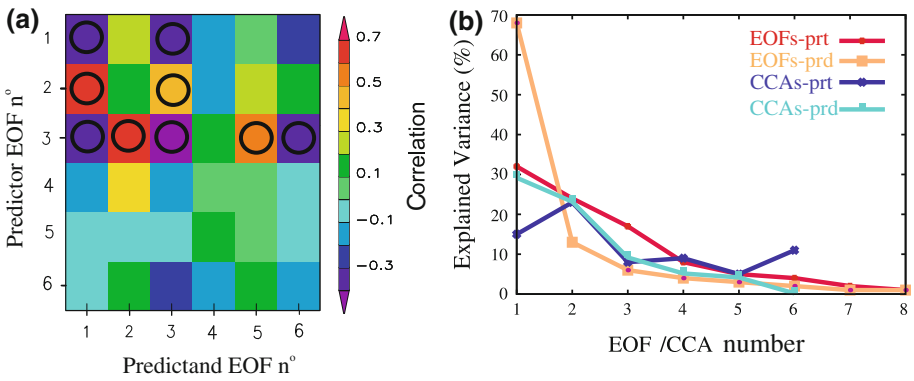

Fig. 9 **a** Correlations between predictor and predictands EOFs. Significant values at a 0.05 level are marked with a *circle*. **b** Explained variance as a function of the number of EOFs/CCAs modes retained for the predictor (*red/blue*) and predictand (*orange/light blue*)

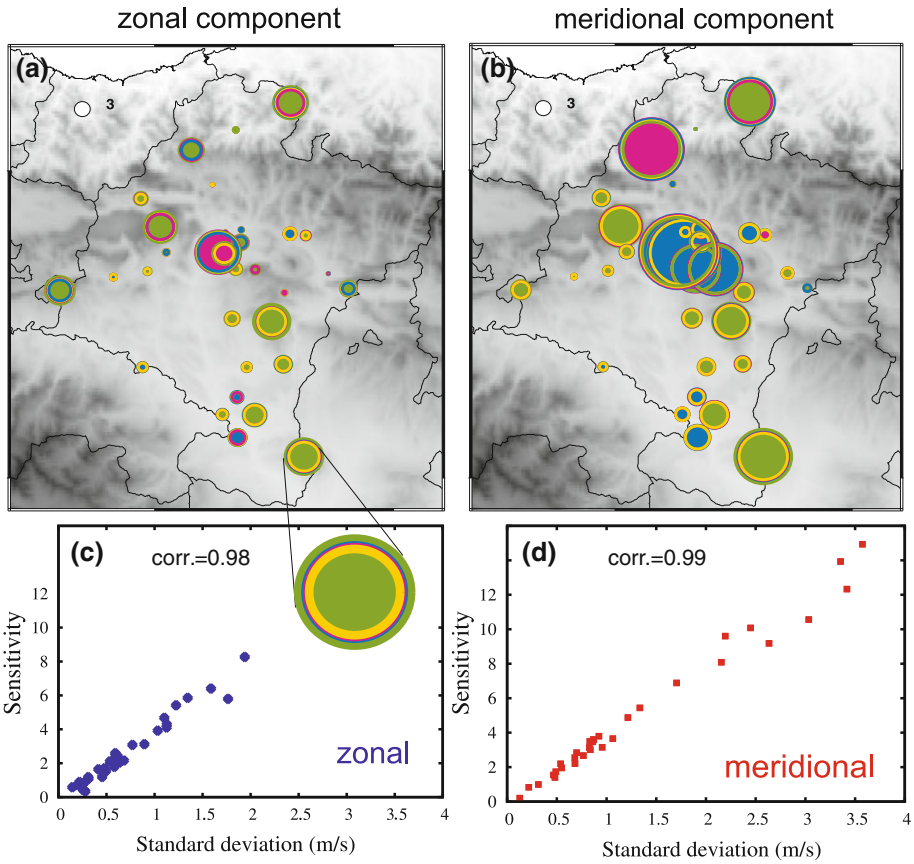

Fig. 10 *Top* Methodological sensitivity at each location in the CFN for the zonal (**a**) and meridional (**b**) wind component, respectively. The size of circumferences is related to the methodological sensitivity obtained in the first step of the uncertainty analysis (only one parameter is allowed to vary at a time in the model). *Colors* indicate what parameter produces the largest contribution to the sensitivity at each location (*green* corresponds to the large scale window, violet to the predictor field, *blue* is associated with the varying number of EOFs/CCAs retained and *yellow* corresponds to the crossvalidation subset size). Bottom: *Sensitivity* at each location in the CFN vs. the corresponding standard deviation of the wind for the zonal (**c**) and meridional (**d**) component

the same criterion of explained variances (see Fig. 9b, note that the explained variance of the predictor is that accounted for by the two combined fields, ϕ_{850} and $Z_{500–850}$). Thus, all possible combinations (31) between the number of EOFs and CCAs in the ranges commented are employed. The crossvalidation time step parameter varies between 1 month and four extended seasons (September to March) so 1–7 (equivalent to 1 year),14 (2 years) and 28 (4 years) months are the crossvalidation subset sizes considered.

Considering the above possibilities, 74 realizations of the model (see Table 4) are obtained. The spatial distribution of the methodological variance is represented in Fig. 10a and b for the zonal and meridional wind component, respectively. The size of the circles at every location is related to the dispersion of the ensemble of estimations: for each time step it is calculated as the difference between the maximum and minimum estimated values and then temporally averaged to obtain a single *sensitivity* value at each site. It can be observed that the circles are larger in the more windy places (the area of the Ebro Valley and the highest mountain sites, see Fig. 2) that also correspond to those locations where the wind speed variability is also larger (Sect. 2.2). This is illustrated by plotting the *sensitivity* at each location (size of circles in Fig. 10a, b) against

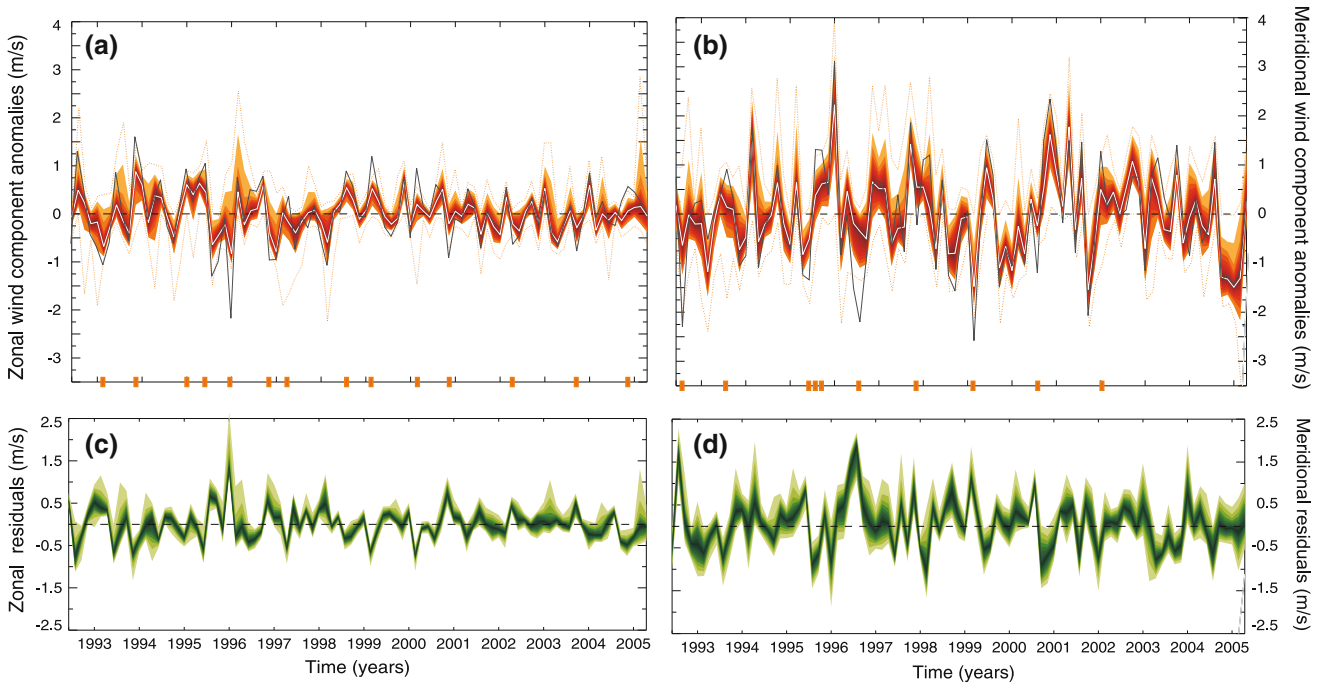

Fig. 11 *Top* Deciles distribution of the regional estimations (*orange*) with respect to the median for **a** the zonal and **b** the meridional wind component together with the observations (*black line*), the reference case estimate (*gray line*, see Sect. 4) and the maximum and minimum values (*dashed orange line*). *Bottom* Deciles distribution of the regional residuals (estimations minus observations) for (**c**) the zonal and (**d**) meridional wind component

the corresponding observed standard deviation of the wind (Fig. 10c and d, zonal and meridional component, respectively). A linear relationship between them is evident. This leads to the conclusion that the larger the standard deviation and thus, the variability of the wind at the specific location, the larger is the sensitivity or associated uncertainty. In these figures it is also evident that the meridional wind component presents higher levels of variability, thus, also a higher sensitivity, compared to the zonal one.

The respective influence of each model parameter has been further analyzed by separating its individual contribution to the spread of estimations. This is done by plotting at each location circumferences with increasing size according to the impact of each parameter in the total uncertainty (Fig. 10a, b). A color code is needed to identify the influence of the variable large scale window (green), the change of predictor field (violet), the varying number of retained EOFs/CCAs (blue) and the crossvalidation subset option (yellow). At each site only the largest circumference is filled with the corresponding color to help in the identification of the parameter that produces larger sensitivity. It can be appreciated that in most parts of the region the size of the large scale domain is responsible for generating the largest uncertainties for the two wind components. There are a few places, especially for the meridional component, where the number of EOFs/CCAs patterns included produce a larger contribution to the uncertainty. However, it is also noticeable that the individual contribution of each parameter is very similar in most of the sites of the region (i.e., similar circumference size, see the zoomed circle in Fig. 10c as an example). In this line, Huth (2002) reported, that the performance of the different predictors were comparable as long as thermal and dynamic fields were included when applying similarly a statistical downscaling approach to estimate daily temperatures over Central Europe.

The interest is focused now in considering the combination of all possible parameter configurations in the design of the experiments, i.e., the parameters described above are allowed to vary jointly in this second step giving rise to a considerably larger number of estimations (more than 60,000, see Table 4). This complements the preliminary methodological sensitivity evaluation in the previous step. The large ensemble obtained is divided in ten groups of equal frequency (deciles) distributed around the median. This is represented for the regional time series in Fig. 11a and b (for the zonal and meridional wind component, respectively) together with the observations (black line), the reference estimate (gray, see Sect. 4) and the maximum and minimum values (dashed orange line). It is interesting to observe that, qualitatively, the uncertainty area preserves the variability of the observations during the whole period 1992–2005, pointing out the robustness of the methodology in estimating the wind field. Thus, most of

the observations are confined within the uncertainty intervals. For illustration, it is shown in the horizontal axis a square-symbol every time the observations exceed the sensitivity area. In the case of the zonal (meridional) component a 15% (9%) of the observations falls out of the area. This percentages agree with the better predictability of the meridional component as explained in Sect. 4.

Thus, the uncertainty represented in Fig. 11a, b evidences that the performance of the model is not largely dependent on the configuration selected and it can be argued that the method is able to reproduce the main features of the surface wind field over the region whatever the selection of the model set up is. The reference estimate maintains to a good degree a centered position within the spread: i.e., the selection of parameters in this case does not yield estimates biased to the tails of the distribution. This suggests that the associations found between the global circulation and the regional wind exposed through the reference case in Sect. 4 are representative of the large number of possible configurations considered in this part of the experiment and also representative of the influence of the synoptic circulation in the regional wind variability.

The deciles distribution of the residuals (estimations minus observations) are shown in Fig. 11c, d for the zonal (meridional) wind component, respectively, for a brief insight into the temporal variation of the errors. No significant trends can be observed neither for the zonal nor the meridional series, pointing that the variance of the residuals is constant along the calibration period, as desired. The structure of the residual series is noisy but still resembles the variability of the observations. As the residuals represent the portion of the observed variance not explained by the model, this points out the existence of a tendency to underestimate the observations variance. A formal residual analysis would include an evaluation of the residual autocorrelation, probability distribution, etc. This is out of the scope of the present study however, a formal treatment of the residuals can be dealt with in future stages of the analysis.

5.2 Single and multi-data experiments

To gain insight into the possible impacts of using different datasets as large scale information entering the model, two comparable experiments are considered. For them the SLP is the single predictor since for some of the datasets this is the only variable available. The rest of parameters is allowed to vary freely as in the previous exercise. The first experiment uses the SLP field from ERA-40 and involves a total of 2511 model configurations. This will be referred hereafter as the single-data experiment. In a second experiment SLP fields from the following datasets were employed (see Table 1): the observed NCAR SLP (Trenberth and Paolino 1980), the Hadley Centre historical SLP (Allan and Ansell, 2006) and the SLP reconstruction for the North Atlantic area by Luterbacher et al. (2002). Similarly every parameter, except for the predictor field is varied in this second case implying a total of 5301 realizations. Note that the Luterbacher et al. (2002) dataset allows only for 5 windows since the westernmost longitude is 30°. This exercise will be referred to as the multi-data experiment through which the effect of using different large scale data resources can be assessed.

The deciles distributions of the ensemble of regional estimates for the single- and multi-data experiments are calculated to account for the sensitivity of estimations to the use of different predictor datasets.

The differences between the two deciles distributions is represented in Fig. 12. Differences for the zonal component present a certain tendency to lower values at the second half of the calibration period (1998–2005) compared to the levels of variance of the first half. This is to a less degree also apparent in the case of the meridional component. These changes in the variance of the regional wind have been already discussed in the view of the canonical series of the previous section and they were attributed to changes in the large scale circulation. Therefore it is apparent that all datasets used capture a fluctuation in the variability of the atmospheric circulation around this period. As a result and in agreement with what was hypothesized in Sect. 5.1, the methodological uncertainties associated with the use of different large scale predictors is larger at the beginning of the observational period since the variability of the regional wind field is also larger during the first years. A closer look at the distribution (boxplots in Fig. 12b, d; blue for the single and violet for the multi-data cases) evidences that these differences are mainly localized in the upper deciles of the distribution, especially the ninth decile. Then, most of the residuals (approx. 80% of the estimations) are close to zero, denoting that no large differences are found from the fact of using different datasets as predictors. In addition, differences between single-data percentile distribution (blue in Fig. 12b, d) and the first case of including variations in all parameters (green; recall that identically only ERA-40 but for more predictor variables were used in the previous subsection) are small since the 90% of values are similarly distributed for both wind components. This supports the previous reasoning of Sect. 5.1 where it was argued that the use of one predictor or combinations of various of them did not cause a very strong impact on the methodological uncertainty.

6 Wind field past variability: a wind climatology reconstruction

The following paragraphs focus on the assessment of the long term past variability, from interannual to decadal or

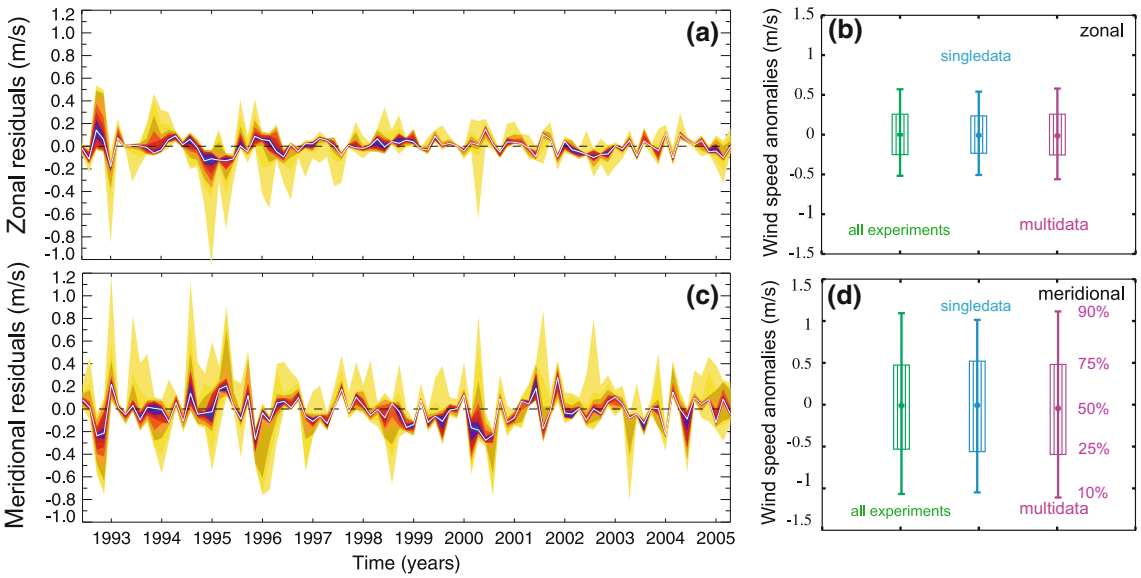

Fig. 12 *Left* Multi-data minus single-data regional residual deciles distribution. *Right* Frequency distribution for the first experiment (variations of all parameters and ERA-40 predictors, Sect. 5.1, *green*), the single-data (*blue*) and the multi-data experiments. **a** and **b** are the zonal and **c** and **d** the meridional wind component

centennial timescales, of the regional wind in the area under study together with the estimation of the long term uncertainties associated with the use of multiple model configurations.

The statistical model derived in Sect. 4 allows for obtaining wind speed estimates when no observations are available out of the calibration period. Similarly, as in Sect. 5.2 regarding the multi-data exercise, the SLP from different datasets is used in the present case as single predictor, yielding past estimations with different temporal coverage (recall Table 1). First, a reference past estimation with each predictor dataset is calculated. For each reference experiment an equal selection of parameters, as the one described in Sect. 4, is considered. Additionally, to make all the experiments comparable the calibration period is fixed to the years between 1992 and 1999, imposed by the time span of the longest SLP dataset (Luterbacher et al. (2002) reconstruction). Thus, the four reference reconstructions differing in their corresponding length and predictor source are labeled as: R_{era40} for the last five decades, R_{ncar} for the 20th century, R_{had2} for the period 1850–2004 and R_{Luterb} for estimates back to the 17th century.

The reference reconstructions of the zonal and meridional regional wind component anomalies are shown in Fig. 13a, b. The associated projected uncertainties related to all possible variations of the model parameters (as in Sect. 5.2, see Table 4) are also presented as deciles distributions in Fig. 13. Some general features of the reconstructed series regarding the long term past variability can be discussed. The meridional component presents also larger variability compared to the zonal one. The negative correlation between the two components also exists at longer time scales as a consequence of the momentum conservation discussed in Sect. 2.2 All reference reconstructions in Fig. 13 show a good temporal concordance in their corresponding overlapping periods and also during the calibration period. It is interesting to observe that a slight discrepancy between the reconstructions takes place in the period from 1850 and 1900, where R_{had2} presents a certain tendency to more negative (positive) anomalies for the zonal (meridional) component compared to R_{Luterb}. This fact suggests the existence of differences in the SLP fields from each data source that were not evident during the observational period (Sect. 5.2). A strengthening or weakening of the large scale patterns in one dataset with respect to the others can be responsible for certain discrepancies between the wind estimates. This issue will be further discussed latter in the present section. Another possibility is that these discrepancies are caused by the presence of certain inhomogeneities in the earlier years of the HadSLP2 dataset due to differences in the density of predictor data in the SLP reconstruction procedure (Allan and Ansell 2006).

Higher anomalous wind velocities can be observed, for instance, in the second half of the 17th and 20th centuries, the first half of the 18th century, the beginning of the 20th century and during the observational period. These larger anomalies (marked with a dashed line in Fig. 13) are especially noticeable in the meridional component of the wind. Regarding the high anomalies during 17th century, previous works address interestingly an increase of wind extremes during the colder period of the Little Ice Age and

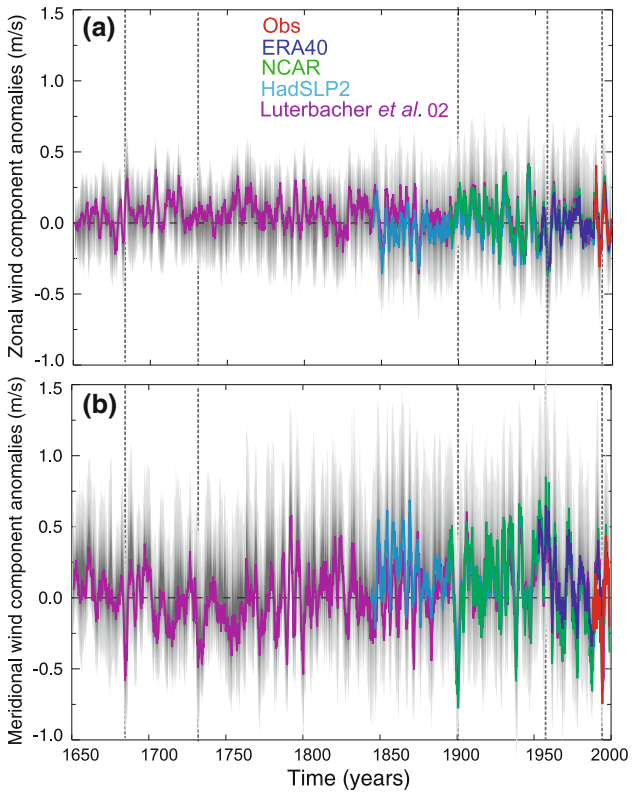

Fig. 13 Wind climatology reconstruction and its associated uncertainty for the zonal (**a**) and meridional (**b**) wind component, respectively. The uncertainty is represented in *gray*. See legends for the *colors* of each driving datasets. Series present a 2 year moving-average filter

especially during the Maunder Minimum (1640–1715) apparently due to a southward shift of the storm tracks between 20°N and 35°N (Raible et al. 2007). However, no significant trends at multicentennial scales are found for the whole reconstruction period. Despite the former, it is apparent the presence of a certain tendency of the zonal (meridional) wind component to positive (negative) values during the second half of the 20th century till present. This can be interpreted as a strengthening of the first canonical mode (Figure 4a) connected with intensification of northwesterly winds over the region. This reinforcement of the meridional circulation was also found by Davis et al. (1996) who detected a trend indicative of such intensification over the eastern Atlantic and western Europe in the second part of the 20th century while exploring the semi permanent subtropical anticyclone and its spatial and temporal variance structure. The reconstructed climatology as well as the projected uncertainty anomalies (gray-shadowed in Fig. 13a, b) reveal the presence of interannual and decadal variability.

The deciles distribution of the uncertainty, similarly to that of the calibration period (Fig. 11) is also represented in Fig. 13a, b (gray shadowed). It can be said that the variability of the past projections of the uncertainty remains in reasonable levels of variance compared to the variance of the reference reconstructions. An insight into the effect that each parameter produces in the long term methodological uncertainty is also discussed. During the observational period the relative importance of the different parameters on the estimated wind was tested. Variations in the predictor field(s), the large scale window, etc., have evidenced a comparable influence in the uncertainty (see Sect. 5.1). However, the question can be posed whether this argument can be considered plausible also for long term variations, or on the contrary, at longer timescales, any of the model parameters has a particular impact on the estimations. To answer this question the estimations are segregated by isolating all cases with a fixed parameter value allowing variations in the rest of parameters of the model configuration in order to investigate the specific influence of each parameter in the reconstructed wind. Only results concerning the number of canonical patterns included in the downscaling model are illustrated (Fig. 14). The uncertainties associated with the estimated wind components have been separated according to the inclusion (orange) or exclusion (gray) of the third and fourth canonical modes. The first situation produces a visible bias to positive (negative) zonal (meridional) anomalies in the earlier years of the reconstruction, while the opposite is true for the case with only two canonical modes (gray in Fig. 14).

The third large scale canonical pattern (CCA3, not shown) consists in a dipole with positive (negative) anomalies over the eastern North Atlantic and a center of opposite sign located to the north of the IP contributing to NE-SW (SW-NE) wind anomalies in the region. This mode is interesting for several reasons. On one hand, the ideal atmospheric situation that generates the Cierzo conditions consists of high surface pressures over England and low ones over the Balearic islands and Italy (de Pedraza 1985), as in the CCA3 large scale pattern in its positive phase. However, the strength of the association of this pattern with the regional wind in the northeastern IP is variable. While small canonical correlations (0.2) and predictand explained variances (5%) are found in the observational period between 1992 and 2005, in the reconstruction exercises, where the statistical model was calibrated between 1992 and 1999, the canonical correlation is 0.66 accounting for a 15% of predictand variance. A test on the sensitivity of the estimations to changes in the calibration interval and length along the observed period was conducted. No impacts were detected due to the slight variations taking place in the intensity of the associations between the local wind and the large scale circulation modes within the observational period. Nevertheless the strength of the large to local scale associations may change depending on the time interval

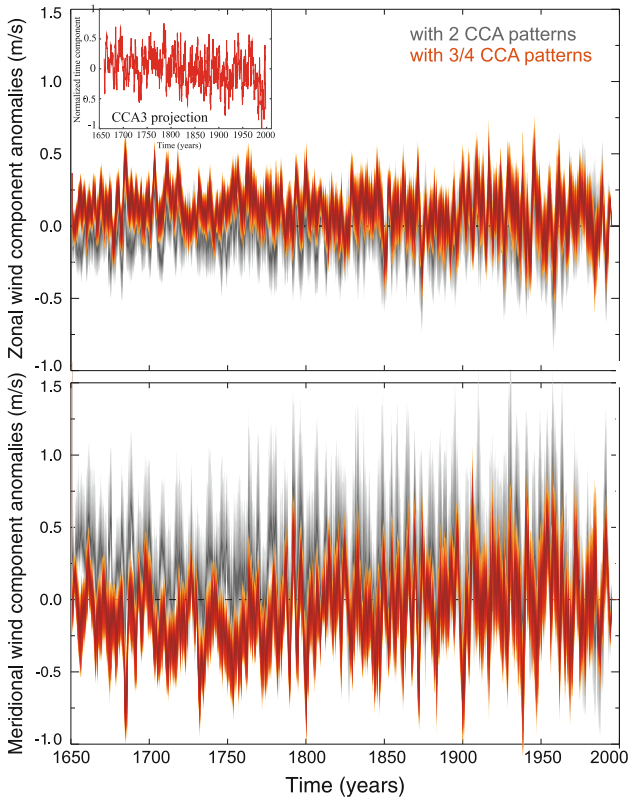

Fig. 14 Uncertainty showing the influence of the inclusion of the third and fourth CCA mode obtained using Luterbacher et al. (2002) SLP reconstruction as predictor for zonal (*top*) and the meridional (*bottom*) wind component. *Gray areas* correspond to the case with only two canonical patterns while orange stands for the cases including the third and fourth patterns. The *inset* in the *top panel* corresponds to the projection on the third canonical series from the middle of 17th century till present obtained using Luterbacher et al. (2002) SLP reconstruction as predictor

considered because of low frequency changes in the modes or in their relative weights (explained variances) throughout the calibration period. This can potentially affect long term estimations of the wind as illustrated in Fig. 14. Even in the case of having relatively long records for calibration (Kaas et al. 1996; Benestad, 2002; Xoplaki et al. 2003a) there is no means of anticipating the occurrence of temporal changes in the associations between the local and the large scales out of the observational period and in fact, this is usually catalogued as the main drawback of statistical models.

An extended estimation of the large scale CCA3 canonical series, calculated applying a regression using Luterbacher et al. (2002) SLP as predictor, is represented in the inset in the top panel of Fig. 14. It is apparent the presence of a tendency towards negative scores which is indicative of a change in sign of the third large scale mode (see Sect. 4.1). This tendency can be considered responsible for the reverse of sign in the past wind estimations depending on the inclusion or not of the third canonical mode, whose contribution to the regional wind is variable. Thus, the apparently negligible impact of selecting a specific number of canonical patterns evidenced during the calibration/validation period, turns out to be of importance in the application of the downscaling model outside of the calibration period. This fact highlights the need for assessing and understanding of the uncertainties associated to the methodology for obtaining downscaling estimates and illustrates that estimations based on a single configuration of the model must be interpreted with care.

7 Summary and conclusions

The analysis of the wind field variability and predictability at the northern Iberian Peninsula is undertaken by applying a statistical downscaling technique, the Canonical Correlation Analysis, to identify the main associations between the regional predictand and the large scale circulation over the North Atlantic area at monthly time scales. To do so, wind measurements from several locations in a complex terrain area at the NE of the IP for the period between 1992 and 2005 have been used.

The two first canonical modes from a certain configuration of the model have been shown as a reference example where the predictor fields (ϕ_{850} and $Z_{500–850}$) are supplied by the ERA-40 reanalysis. The modes of variability found highlight the meridional component of the flow as preferred direction of the regional wind together with the strong influence of the surrounding orography as the Ebro Valley, which serves as a natural channel that accelerates the flow. The wind field is represented as a linear combination of the leading synoptic patterns governing the regional circulation. The approach has proven skillful after comparison of the estimations with the observed wind during the crossvalidation process.

Results evidence a certain underestimation of the variance that can be attributed to the linear constraint imposed by the method in the search of associations between the regional and the synoptic circulations. Thus, there is space for the study of alternative approaches that do not emphasize the linearity in the methodology. In addition, non-linear processes that resolve in shorter than monthly timescales are filtered out here. They may also contribute to some extent to the wind variability underestimation. This calls for the investigation of these type of statistical downscaling methods at, for instance, daily timescales, in order to test their skill in reproducing higher frequency wind variability.

The methodological sensitivity has been evaluated by allowing individual variations of the model parameters values. This exploration illustrates that the uncertainty associated with the method depends on the variability of

the wind at each specific location. In a second step multiple experiments are carried out in which changes in the different parameters of the model configuration are systematically combined yielding a very large number of estimates (more than 60,000). The uncertainty that is associated to this part of the analysis remains in the range of the variability of the observations and also shows a large dependence on the wind field variance. A full assessment of the uncertainty in the downscaling step is provided by considering the influence in estimations of using different data sources as large scale predictors namely, reanalysis, observations as well as a proxy-based reconstruction. The results are illustrative of a discrete influence of this type of uncertainty showing the largest impacts in the upper deciles of the estimates uncertainty distribution. However, the type of large scale predictor introduces more uncertainty which adds to that generated by the variation of the parameters in the downscaling model. In view of the uncertainty obtained, the statistical method appears as a robust approach to estimate the monthly wind in this region.

The long term past variability of the regional wind has been assessed by a regression-based approach fed by the information from the large scale circulation in the absence of observed measurements out of the calibration period. Different data sources are employed and the comparison between the independent wind estimations revealed a good agreement during the overlapping periods. No overall trends along the approx. 350 years of wind reconstruction are appreciated, though signs of considerable interannual and interdecadal variability are found. Uncertainties were also projected backward to gain insight into the degree of dispersion of wind estimations in the past due to the methodological variance and to illustrate the potential impact of using different datasets as synoptic circulation predictors. In this context, the long term variability of the regional wind field revealed a special sensitivity to the choice of the method configuration. Specifically, the presence of a trend found in the canonical series of one of the modes produced clear tendencies of opposite sign in the regional estimated wind, depending on the inclusion or not of the third and fourth modes in the model. This type of exercises allows for the assessment of fluctuations in the regional wind and its main drivers at climatic scales which could be of great value in the context of for instance, wind power production sustainability.

The comparison among the different types of uncertainty associated with regional wind estimates could represent a valuable exercise that can be extended for instance to the context of future climate projections. This would allow for the comparison of the uncertainties obtained in the downscaling step to those associated to a changing of the driving climate model output or the forcing scenario.

Acknowledgments The authors are grateful for the interesting discussions and valuable comments to Dr. D. Bray, Dr. A. Gershunov, Dra. A. Hidalgo, Dr. J. Luterbacher, Dra. M. Montoya, Dr. C. Raible, Dr. P. D. Sardeshmukh, Dr. D. Stephenson, Dr. S. Wagner and Dr. E. Zorita. We acknowledge Dr. Luterbacher for providing the SLP reconstructions back to 1650 and the MedCLIVAR organization for providing the ESF grant that allowed for a stay at the University of Bern, Switzerland. We thank Acciona Energía for facilitating the wind farms dataset. We are also grateful to the ECMWF for providing the ERA-40 data and the outputs from the operational model used in this research. We acknowledge the working framework established by the collaboration between CIEMAT and the PalMA group at UCM (Ref. 09/153). Part of the financial support for some of the authors involved in this work was provided by the projects CGL2005-06966-C07/CLI, PSE-120000-2007-14 and CGL2008-05093/CLI. The authors wish to thank the two anonymous reviewers for their comments and suggestions.

References

Allan R, Ansell T (2006) A new globally complete monthly historical gridded mean sea level pressure dataset (HadSLP2): 18502004. J Clim 19:5816–5842

Barnett TP, Preisendorfer RW (1987) Origin and levels of monthly and seasonal forecast skill for United States air temperature determined by canonical correlation analysis. Mon Wea Rev 115:1825–1850

Barnston A, Livezey R (1987) Classification, seasonality and persistence of low-frequency atmospheric circulation patterns. Mon Wea Rev 115(6):1083–1116

Benestad R (2002) Empirical downscaled temperatue scenarios for northern Europe based on a multi-model ensemble. Clim Res 21:105–125

Bianco L, Tomassetti E, Coppola E, Fracassi A, Verdecchia M, Visconti G (2006) Thermally driven circulation in a region of complex topography: comparison of wind-profiling radar measurements and mm5 numerical predictions. Ann Geophys 24:1537–1549

Burlando M (2009) The synoptic-scale surface wind climate regimes of the Mediterranean sea according to the cluster analysis of ERA-40 wind fields. Theor Appl Climatol 96:69–83

Busuioc A, Tomozeieu R, Cacciamani C (2008) Statistical downscaling model based on canonical correlation analysis for winter extreme precipitation events in the Emilia-Romagna region. Int J Climatol 28(4):449–464

Buzzi A, D'Isidoro M, Davolio S (2003) A case study of an orographic cyclone south of the Alps during the mAP SOP. Q J R Meteorol Soc 129:1795–1818

Caires S, Sterl A (2004) 100-year return value estimates for ocean wind speed and significant wave height from the ERA-40 data. J Clim 18:1032–1048

Conil S, Hall A (2006) Local regimes of atmospheric variability: a case study of southern california. J Clim 19-17:4308–4325

Davis R, Hayden B, Gay D, Phillips W, Jones G (1996) The North Atlantic subtropical anticyclone. J Clim 10:1788–1806

Denman K, Brasseur G, Chidthaisong A, Ciais P, Cox P, Dickinson R, Hauglustaine D, Heinze C, Holland E, Jacob D, Lohmann U, Ramachandran S, da Silva Dias P, Wofsy S, Zhang X (2007) Couplings between changes in the climate system. In: Solomon S et al (eds.) Climate change 2007: the physical science basis. Contribution of working group I to the fourth assessment report of the intergovernmental panel on climate change. Cambridge University Press, Cambridge

Dibike Y, Gachon P, St-Hilaire A, Ouarda T, Nguyen VTV (2008) Uncertainty analysis of statistically temperature and

precipitation regimes in northern Canada. Theor Appl Climatol 91:149–170
Fernández J, Saenz J (2003) Improved field reconstruction with the analog method: searching the CCA space. Cli Res 24:199–213
Fernández J, Montávez J, Saenz J, González-Rouco J, Zorita E (2007) Sensitivity of the MM5 mesoscale model to physical parameterizations for regional climate studies: annual cycle. J Geophys Res 112. doi:10.1029/2005JD006,649
Fisher E, Seneviratne I, Lüthi D, Schär C (2007) Contribution of land-atmosphere coupling to recent European summer heat waves. Geophys Res Lett 34:L06,707
Furrer R, Sain S, Nychka D, Meehl G (2007) Multivariate bayesian analysis of atmosphere-ocean general circulation models. Environ Scol Stat 14:249–266
García-Bustamante E, González-Rouco JF, Jiménez PA, Navarro J, Montávez JP (2008) The influence of the Weibull assumption in monthly wind. Wind Ener 11:483–502
García-Bustamante E, González-Rouco JF, Jiménez PA, Navarro J, Montávez JP (2009) A comparison of methodologies for monthly wind energy estimations. Wind Ener 12:640–659
Gerstengarbe BOFW, Werner P (2008) A resampling scheme for regional climate simulations and its performance compared to a dynamical RCM. Theor Appl Climatol 92:209–223
Glahn H (1968) Canonical correlation and its relationship to discriminant analysis and multiple regression. J Atmos Sci 25:23–31
González-Rouco J, Heyen H, Zorita E, Valero F (2000) Agreement between observed rainfall trends and climate change simulations in the southwest of Europe. J Clim 13:3057–3065
Grimenes A, Thue-Hansen V (2004) Annual variation of surface roughness obtained from wind profiles measurements. Theor App Climatol 79(1-2):93–102
Hanssen-Bauer I, Achberger C, Benestad R, Chen D, Førland E (2005) Statistical downscaling of climate scenarios over Scandinavia. Clim Res 29:255–268
Hong S, Kalnay E (2000) Role of sea surface temperature and soil-moisture feedback in the Oklahoma-Texas drought. Nat Biotechnol 408(6814):842–844
Hotelling H (1935) The most predictable criterion. J Educ Psychol 26:139–142
Hotelling H (1936) Relations between two sets of variables. Biometrika 28:321–377
Huth R (2000) Statistical downscaling in Central Europe: evaluation of methods and potential predictors. Clim Res 13:91–101
Huth R (2002) Statistical downscaling of daily temperature in Central Europe. J Clim 1:1731–1742
Huth R (2004) Sensitivity of local daily temperature change estimates to the selection of downscaling models and predictors. J Clim 17:640–652
Jakobs H, Feldman H, Hass H (1995) The use of nested models for air-pollution studies—an application of the EURAD model to a SANA episode. J Appl Meteorol 34(6):1301–1319
Jiménez PA, González-Rouco JF, Montávez JP, García-Bustamante E, Navarro J (2008a) Climatology of wind patterns in the Northeast of the Iberian Peninsula. Int J Climatol 29:501–525
Jiménez PA, González-Rouco JF, Montávez JP, Navarro J, García-Bustamante E, Valero F (2008b) Surface wind regionalization in a complex terrain region. J Appl Meteorol Clim 47:308–325. doi:10.1175/2007JAMC1483.1
Jiménez PA, González-Rouco JF, García E, Montávez JP, García-Bustamante E, Navarro J (2010a) Quality-control and bias correction of high resolution surface wind observations from automated weather stations. J Atmos Oceanic Tech A 27:1101–1122
Jiménez PA, González-Rouco JF, García-Bustamante E, Navarro J, Montávez JP, de Arellano JVG, Dudhia J, Roldán A (2010b) Surface wind regionalization over complex terrain: evaluation and analysis of a high resolution WRF numerical simulation. J Appl Meteorol Climatol 49:268–287
Kaas E, Li T, Schmith T (1996) Statistical hindcast of wind climatology in the North Atlantic and northwestern European region. Clim Res 7:97–110
Kaiser H (1960) The application of electronic computers to factor analysis. Educ Psychol Mesure 20:141–151
Kariniotakis G, Pinson P, Siebert N, Giebel G, Barthelmie R (2004) The state of the art in short-term prediction of wind power-from an offshore perspective. In: Proceedings of 2004 SeaTech Week
Koukidis EN, Berg AA (2009) Sensitivity of the statistical downscaling model (SDSM) to reanalysis products. Atmos Ocean. doi:10.3137/AO924.2009
Lenderink G, van Ulden A, van den Hurk B, Keller F (2007) A study on combining global and regional climate model results for generating climate scenarios of temperature and precipitation for the Netherlands. Clim Dyn 32:157–176
Levine M (1977) Canonical analysis and factor comparison. Sage University Publications, Beverly Hills
Luterbacher J, Xoplaki E, Dietrich D, Rickli R, Jacobeit J, Beck C, Gyalistras D, Schmutz C, Wanner H (2002) Sea level pressure fields over the eastern North Atlantic and Europe back to 1500. Clim Dyn 18:545–561
Matulla C, Scheifinger H, Menzel A, Koch E (2003) Exploring two methods for statistical downscaling of Central Europe phenological time series. Int J Biometeorol 48:56–64
Maurer EP, Hidalgo HG (2007) Utility of daily vs. monthly large-scale climate data: an intercomparison of two statistical downscaling methods. Hydrol Earth Syst Sci Discuss 4:3413–3440
McKendry I, Stahl K, Moore R (2006) Synoptic sea-level pressure patterns generated by a general circulation model: Comparison with types derived from NCEP/NCAR re-analysis and implications for downscaling. Int J Climatol 26:1727–1736
Michaelsen J (1987) Cross-validation in statistical climate forecast models. J Clim App Meteorol 26:1589–1600
Mitchell T, Hulme M (1999) Predicting regional climate change: living with uncertainty. Prog Phys Geograph 23(1):57–78
Najac J, Boé J, Terray L (2009) A multi-model ensemble approach for assessment of climate change impact on surface winds in france. Clim Dyn 32:615–634
Nakicenovic N, Alcamo J, Davis G, de Vries B, Fenhann J, Gaffin S, Gregory K, Grübler A et al (eds) (2000) Special report on emissions scenarios. Working group III, intergovernmental panel on climate change (IPCC). Cambridge University Press
North G, Bell T, Calahan R, Moeng F (1982a) Sampling errors in the estimation of empirical orthogonal functions. Mon Wea Rev 110:699–706
North G, Moeng F, Bell T, Calahan R (1982b) The latitude dependence of the variance of zonally averaged quantities. Mon Wea Rev 110:319–326
de Pedraza LG (1985) La predicción del Tiempo en el Valle del Ebro. Technical Report Serie a. Technical report 38, INM
Powell M, Dodge P, Black M (1991) The landfall of hurricane hugo in the carolinas-surface wind distribution. Wea Forecast 6(3):379–399
Preisendorfer R (1988) Principal component analysis in meteorology and oceanography. Elsevier, Amsterdam
Pryor S, Schoof J (2005) Empirical downscaling of wind speed probability distributions. J Geophys Res 110:D19,109
Pryor S, Barthelmie R, Kjellström E (2005a) Potencial climate change impact on wind energy resources in northern Europe: analyses using a regional climate model. Clim Dyn 25:815–835
Pryor S, Schoof J, Barthelmie RJ (2005b) Climate change impacts on wind speeds and wind energy density in northern Europe:

empirical downscaling of multiple AOGCMs. Clim Res 29:183–198

Pryor S, Schoof J, Barthelmie R (2006) Winds of change? Projections of near-surface winds under climate change scenarios. Geophys Res Lett 33:L11,702. doi:10.1029/2006GL026,000

Pryor S, Barthelmie R, Tackle G (2009) Wind speed trends over the contiguos usa. IOP Conference Series: Earth Environ Sci 6. doi: 10.1088/1755–1307/6/9/092,023

Raible C, Yoshimori M, Stocker T, Casty C (2007) Extreme midlatitude cyclones and their implications for precipitation and wind extremes in simulations of the Maunder Minimum versus present day conditions. Clim Dyn 28:409–423

de Rooy W, Kok K (2004) A combined physical-statistical approach for the downscaling of model wind speed. Weather Forecast 19:485–495

Schwierz C, Appenzeller C, Davies H, Liniger M, Muller W, Stocker T, Yoshimori M (2006) Challenges posed by and approaches to the study of seasonal-to-decadal climate variability. Clim Change 79

Seierstad IA, Stephenson D, Kvamstö N (2007) How useful are teleconnection patterns for explaining variability in extratropical storminess. Tellus 59:170–181

Simpson J (1994) Sea breezes and local winds. Cambridge University Press, Cambridge

von Storch H (1995) Inconsistencies at the interface of climate impact studies and global climate research. Meteorol Zeitschrift 4:71–80

von Storch H, Zwiers F (1999) Statistical analysis in climate research. Cambridge University Press, Cambridge

von Storch H, Zorita E, Cubasch U (1993) Downscaling of global climate change estimates to regional scales: an application to Iberian rainfall in wintertime. J Clim 6:1161–1171

Taylor K (2001) Summarizing multiple aspects of model performance in single diagram. J Geophys Res 106:7183–7192

Trenberth K, Paolino D (1980) The northern hemisphere sea level pressure dataset: trends, errors and discontinuities. Mon Wea Rev 108:856–872

Uppala S, Kallberg P, Simmons A, Andra U, daCosta Bechtold V, Fiorino M, Gibson J, Haseler J, Hernandez A, Kelly G, Li X, Onogi K, Saarinen S, Sokka N, Allan R, Andersson E, Arpe K, Balmaseda M, Beljaars A, van de Berg L, Bidlot J, Bormann N, Caires S, Chevallier F, Dethof A, Dragosavac M, Fisher M, Fuentes M, SHagemann EEH, Hoskins B, Isaksen L, Janssen P, Jenne R, McNally A, Mahfouf J, Morcrette J, Rayner N, Saunders R, Simon P, Sterl A, Trenberth K, A AU, Vasiljevic D, Viterbo P, Woollen J (2005) The era-40 re-analysis. Q J R Meteorol Soc 131:2961–3012

Weisse R, Feser F (2003) Evaluation of a method to reduce uncertainty in wind hindcasts performed with regional atmosphere models. Coast Eng 48:211–225

Xoplaki E, González-Rouco J, Gyalistras D, Luterbacher J, Rickli R, Wanner H (2003a) Interannual summer air temperature variability over Greece and its connection to the large-scale atmospheric circulation and Mediterranean SSTs 1950-1999. Clim Dyn 20:537–554

Xoplaki E, González-Rouco J, Luterbacher J (2003b) Mediterranean summer air temperature variability and its connection to the large-scale atmospheric circulation and SSTs. Clim Dyn 20:723–739

Xoplaki E, González-Rouco JF, Luterbacher J, Wanner H (2004) Wet season Mediterranean precipitation variability: influence of large-scale dynamics and predictability. Clim Dyn 23:63–78

Zhang D, Zheng W (2004) Diurnal cycles of surface winds and temperatures as simulated by five boundary layer parametrizations. J Appl Meteorol 43:157–169

Zhang N, Jiang W, Miao S (2006) A large eddy simulation on the effect of buildings on urban flows. Wind Struct 9(1):23–25

Zorita E, von Storch H (1999) The analog method as a simple statistical downscaling technique: comparison with more complicated methods. J Clim 12:2474–2489

Zorita E, Viacheslav K, von Storch H (1992) The atmospheric circulation and sea surface temperature in the North Atlantic area in winter: their interaction and relevance for Iberian precipitation. J Clim 5:1097–1108